ADDRESSABLE MICROLENS ARRAY TO IMPROVE DYNAMIC RANGE OF SHACK-HARTMANN SENSORS

Hyuck Choo and Richard S. Muller
Berkeley Sensor & Actuator Center
Department of Electrical Engineering and Computer Sciences
University of California at Berkeley
Berkeley, California 94720-1774 USA

ABSTRACT

We demonstrate an addressable array (5-by-5) of high-quality microlenses applied to a Shack-Hartmann (SH) sensor in a micro-optical system. Specific lenses in the array can be addressed using a new selection scheme (that we have designed, built, and tested) in which the mechanical resonant frequencies of individual lens-support carriages are varied. Thus, by changing the frequency of the drive voltage, we require only two electrical connections per row in the lens system to identify the selected lens by its resonating focal image. We show that using this lens-identification method allows us to improve the dynamic range of Shack-Hartmann sensors by 2600-4600% over values attained in conventional SH designs.

INTRODUCTION

Shack-Hartmann sensors are widely used in astronomical telescopes and ophthalmic-analysis systems as monitors for wavefront aberrations. They are fast, accurate and, in contrast to interferometers, generally insensitive to vibrations. When used in conjunction with adaptive mirrors, Shack-Hartmann sensors are able to improve the image quality of astronomical telescopes by performing real-time corrections on the wavefront aberrations that are inherently generated as starlight traverses the earth's atmosphere.

In Shack-Hartmann systems, a microlens array dissects an incoming wavefront into a number of segments (Figure 1). Each microlens in the array creates a focal spot within the assigned sub-aperture on the CCD (typically made of 40 CCD pixels). Because light travels in a straight path normal to the wavefront, the position of these focal spots is related to the average wavefront slope over each microlens aperture. Thus the pattern of spots at the focal plane contains information about the spatially-resolved waveform slope that can be integrated to reconstruct the wavefront [1]. The dynamic range (the range of measurable wavefront slope/curvature) of a conventional SH system has fundamental design limits that must be kept in mind; a SH system produces false results if the curvature or the slope of the wavefront being measured is too large. Figure 2 shows one of such cases in which a focal point of one microlens dislocates into an adjacent sub-aperture assigned to a focal point of another microlens.

Researchers have attempted to overcome this dynamic-range limitation of SH systems using at least three methods: (1) employing a modified unwrapped algorithm,(2) using a SH array of microlenses with well-defined astigmatism, or (3) positioning a spatial-light modulator in front of the SH microlens array as a shutter [2-4]. Research showed that the first two methods had very limited practical use because they worked only with certain types of wavefronts. Method (1) works with highly sloped planar wavefronts but not with highly curved wavefronts. Method (2) fails if the incoming light contains astigmatic characteristics, possibly canceling out the well-defined astigmatism of the lens array and thereby making it impossible to identify where the focal points come from. Method (3) which employs a spatial-light modulator is also impractical on three grounds: the modulator absorbs a great deal of light (at least 50% in the case of an LCD illuminated with unpolarized light); it increases the noise in the measurement; and it introduces additional aberrations to the wavefront being measured. In addition, spatial-light modulators may have polarization dependences, and they are typically very expensive.
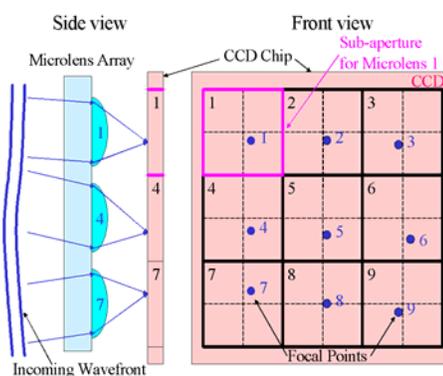

Figure 1. *Wavefront-slope measurement using microlens array: Each microlens has its own sub-aperture consisting of forty CCD pixels (divided into four quadrants), and the focal point of the microlens must be located within the assigned sub-apertures*
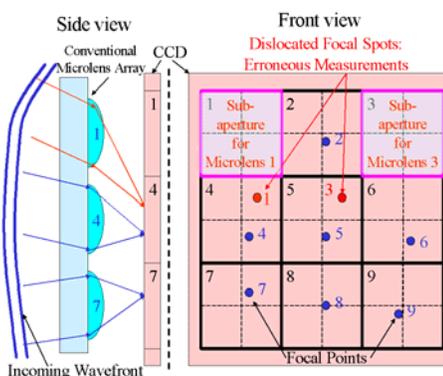

Figure 2. *Limited dynamic range of a conventional Shack-Hartmann sensor (left): A highly curved- or steeply sloped-wavefront causes the focal points of microlenses #1 and #3 to mis-locate onto the sub-apertures assigned to microlenses #4 and #5, respectively, causing erroneous measurements.*

Using MEMS technologies developed in the Berkeley Microlab, we have created densely packed active microlens arrays that are individually controlled to resonate at given frequencies. When a lens resonates, its focal point will move parallel to it; hence by energizing one microlens, we identify its focal point

through its movement (Figure 3). We have varied the mechanical resonant frequencies of individual lens-support carriages so that, by changing the frequency of the drive voltage, we require only two electrical connections per row in the lens system to identify the selected lens. Figure 4 shows a schematic diagram of a microlens array and an enlarged view of an active MEMS microlens unit. Through our design, a lens focal point can be identified outside its associated sub-aperture (usually 40 pixels), anywhere in the sensing array. This identification allows the dynamic range of the SH sensor to be dramatically improved-- a factor of 26 to 46 better than that achieved in conventional Shack-Hartmann systems.
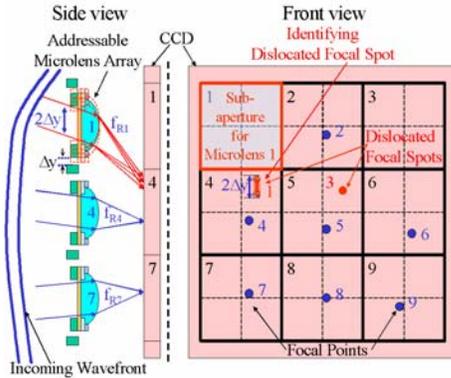

Figure 3. *By making each microlens resonate individually, we can identify its associated focal point, even if the focal point is located outside the assigned sub-aperture.*
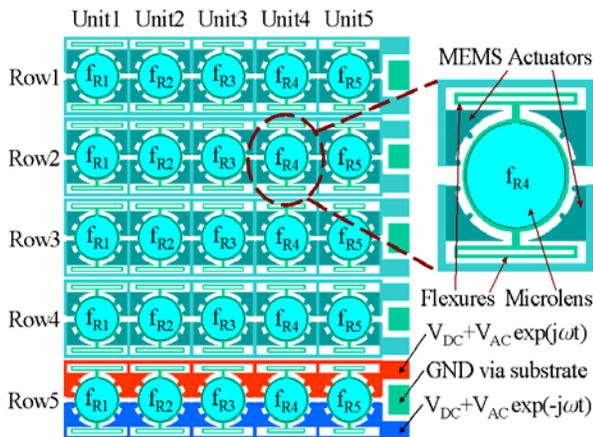

Figure 4. *Schematic diagram of addressable microlens array: Our resonant-frequency addressing method requires only a single pair of electrical lines per row to control each unit individually.*

DESIGN CONSIDERATIONS AND FABRICATION

Our addressable microlens array for Shack-Hartmann sensors has been based on the following design principles: 1. Maximizing the clear aperture of the system (or microlens area) by minimizing the areas for actuators and interconnects; 2. Reducing mechanical cross-talk between different units as much as possible in order to avoid errors in identifying a lens 3. Assuring that only the desired lens moves appreciably even when it must be actuated with the highest driving voltage for lenses in its row. The resonant frequency of each structure is varied by decreasing the support-flexure lengths from 900 to 500 μm in steps of 100 μm. Theoretical analysis of the system predicts that when one of the

units is at full resonance of ±20 μm, the other four units move less than a few microns.

Our 5×5 addressable-lens arrays, fabricated using SOI wafers, are pictured in the SEM photographs shown in Figure 6-9. Each addressable unit (1.5mm square) contains one 800μm-diameter microlens with lens-support carriage and actuators. The microlenses are precisely formed using our polymer-jet printing technology (described earlier [5]) within the 20μm-deep circular wells (etched in the device layers of SOI wafers) having 2μm-thick silicon-nitride-membrane floors. The boundaries of the circular wells define the lens diameters, and the polymer surface tension creates a high-quality optical surface. Figure 5 illustrates the processing steps. The buried- oxide mask is used in order to pattern fine features such as comb fingers and flexures after creating 20μm-deep contact holes and circular wells. The handling layer is also used as electrical ground, and the moving structures are electrically connected to the handling layer through the contacts, preventing any unwanted electrostatic pulling forces.
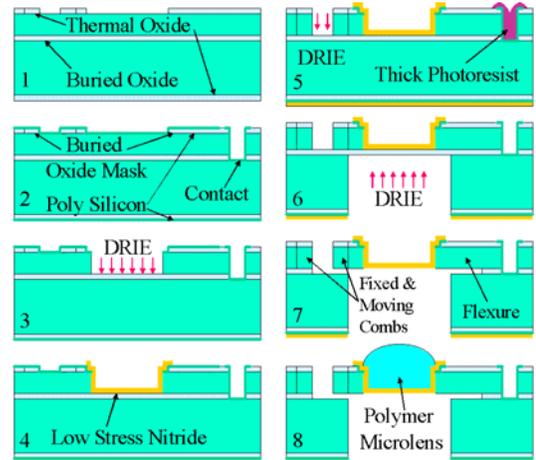

Figure 5. *Fabrication process: **1**. Grow 1μm-thick thermal oxide on a SOI wafer. Define combs, flexures, supports, and lens frames to make buried oxide-layer mask; **2**. DRIE halls and deposit 0.5μm-thick LPCVD poly-Si layer to create electrical contacts from the device layer to the handling layer (GND). Poly-Si layer also protects the oxide mask; **3**. DRIE circular trenches in the device layer; **4**. Deposit and pattern silicon nitride layer (tensile stress, ~250MPa); **5**. DRIE silicon parts (combs, flexures, supports, and lens frame) using the buried oxide mask; **6**. Open the backside of the lens using DRIE; **7**. HF Release; **8**. Make microlenses using polymer-jet printing technology. The boundary of the trench defines the diameter of the lens.*
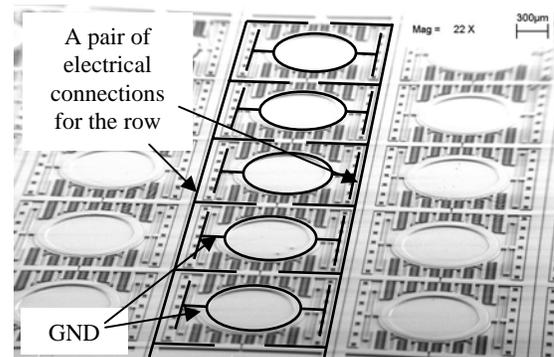

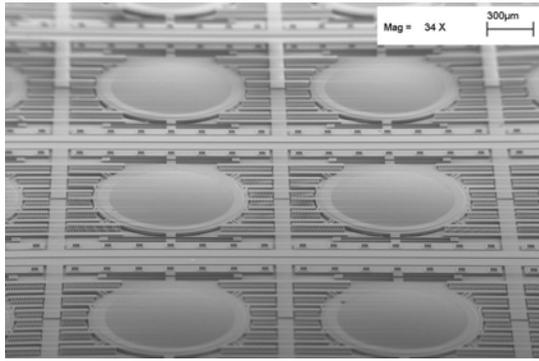**Figure 6.** *SEM picture of the fabricated addressable microlens array before microlens fabrication*

Figure 7. *SEM picture of the fabricated addressable microlens array before microlens fabrication*
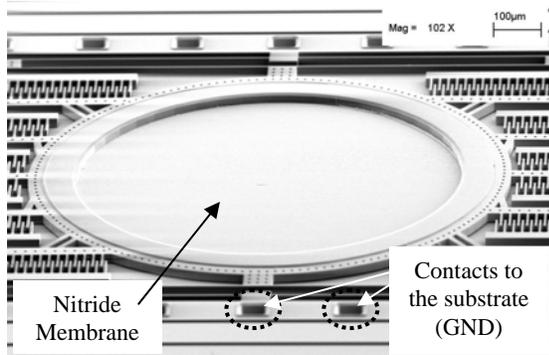

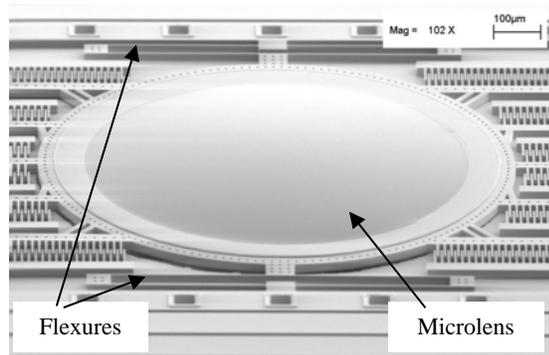**Figure 8.** *SEM picture of the fabricated addressable microlens unit before microlens fabrication*

Figure 9. *SEM picture of the fabricated addressable microlens unit after microlens fabrication*

EXPERIMENTAL RESULTS

Polymer-jet printing technique in circular wells has produced microlenses with effective focal lengths (EFL) ranging from 1.94 to 7.48mm as adjusted by controlling the volume of the microlenses. Twenty-five microlenses (average EFL=2.09mm), fabricated using this method, showed ≤5% variation (peak-to-peak) in EFL. Using WYKO-NT3300, we measured the surface profiles of the low-stress (~250MPa) tensile-nitride-membranes and microlenses (EFL=5.5mm) (Figure 10). Within a 200μm-radius, the membranes are virtually flat (radius-of-curvature≥3m) and the microlenses closely follow an ideal circle (radius=2.2mm).

The measured mechanical resonant frequencies of the MEMS-microlens units 1 through 5 with {without} microlenses (EFL=2.09mm) are 0.654{2.03}, 0.789{2.46}, 0.989{3.06},

1.241{4.08}, and 1.744{5.43} kHz (Figure11). The corresponding Q-factors with {without} microlenses (EFL=2.09mm) are 65.4{18.5}, 105.1{24.6}, 142.1{30.6}, 174.8{58.3}, and 205.2{90.5} (Figure12). The maximum variation of resonant frequencies between rows is approximately 5 % {2 %}. All units achieve 40μm resonant excursions (±20μm) when applying actuation voltages (|VAC+VDC|) lower than 50V (Figure13). Figure14 shows an optical demonstration of microlens identification and its associated focal point using our scheme. We have only observed mechanical crosstalk between units 1 and 4. When unit 4 is resonating with amplitude of 40μm, the unit-1 lens shows an approximately 3μm-oscillation, which is too small to cause identification error.

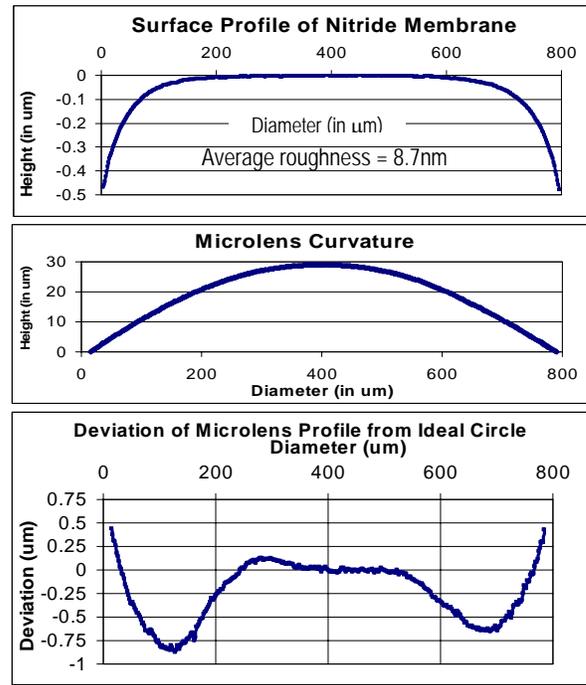**Figure 10.** *Low tensile-stress (250MPa) nitride membrane is very flat (radius of curvature≥3m) within 200μm radius. Its profile deviates from an ideal flat surface near the edge. The microlens (f=5.5mm) profile follows closely with an ideal circle (radius=2.2mm) within 200μm radius. Its deviation near the edge may be influenced by the profile of the nitride membrane underneath it.*

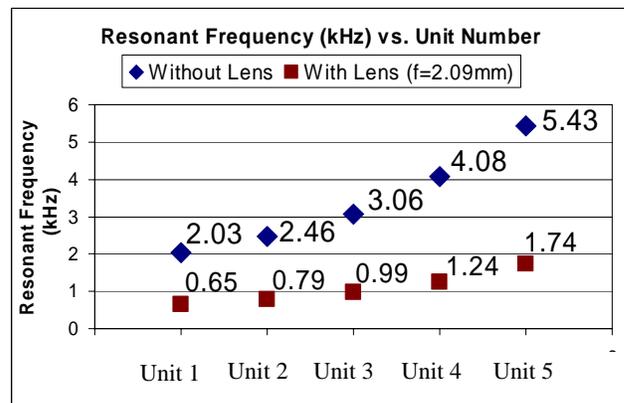**Figure 11.** *Resonant frequencies of the fabricated addressable microlens array before and after microlens fabrication*

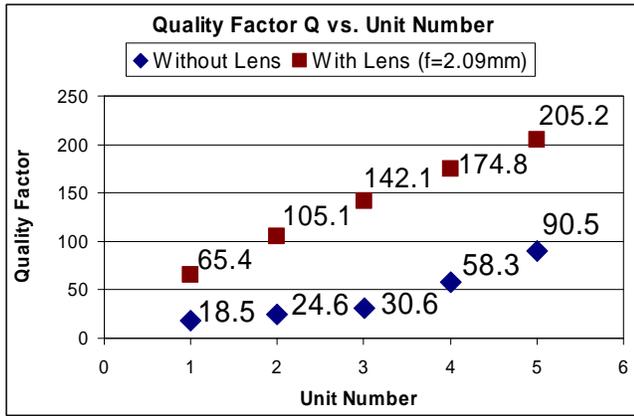## Quality Factor Q vs. Unit Number

Figure 12. *Q-factors of the fabricated addressable microlens array after microlens fabrication*
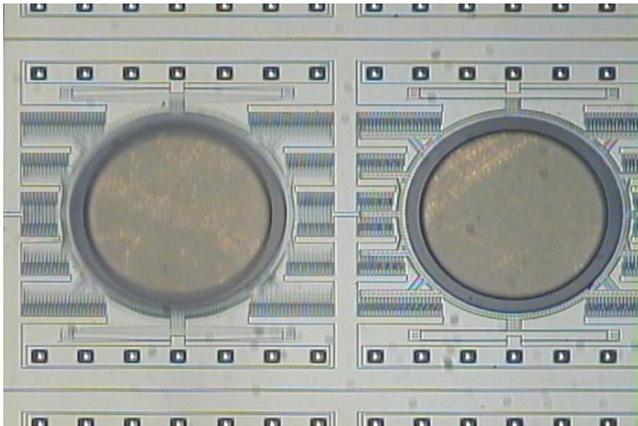

Figure 13. *Unit1 (left) is at resonance. All other units in the row show no movement. Non-uniform metallic texture seen on the nitride membrane is a reflection of the surface of the copper wafer-chuck of the optical microscope.*

Figure 14. *Demonstration of focal point identification: As the microlens resonates, its focal point turns into a scanning line, and the focal point and its associated microlens can be identified. The focal length f of the microlens is 2.09mm, and the CCD imager is placed at 9.84f from the lens. The focal point travels 40μm×9.84f or 0.3936mm on the CCD imager.*

CONCLUSIONS

We have demonstrated an addressable array (5-by-5) of high-quality microlenses which can be applied to a Shack-Hartmann (SH) sensor in a micro-optical system to improve its dynamic range. Specific lenses in the array can be addressed using our new design in which the mechanical resonant frequencies of individual lens-support carriages are varied. The measured mechanical resonant frequencies of the MEMS-microlens units 1 through 5

with {without} microlenses (EFL=2.09mm) range from 0.654{2.03}, up to 1.744{5.43} kHz. The corresponding Q-factors with {without} microlenses (EFL=2.09mm) were between 65.4{18.5} and 205.2{90.5}. All units achieve 40μm resonant excursions (±20μm) when applying actuation voltages ($|V_{AC}+V_{DC}|$) lower than 50V. Optically observed mechanical cross-talk between different units was negligible. The frequency selection of MEMS structures that is demonstrated in this project has clear advantages for other applications.

REFERENCES

1. D. R. Neal, E. Hedlund, M. Lederer, A. Collier, C. Spring, and W. Yanta, "Shack-Hartmann wavefront sensor testing of aero-optic phenomena," *20th AIAA Advanced Measurement and Ground Testing Technology Conference*, June 15-18, 1998, pp.2-13

2. J. Pfund, N. Lindlein, J. Schwider, "Dynamic range expansion of a Shack-Hartmann sensor by use of a modified unwrapping algorithm," *Optics Letters, vol.23, no.13,* July 1998, pp.995-7. Opt. Soc. America, USA.

3. N. Lindlein, J. Pfund, J. Schwider, "Expansion of the dynamic range of a Shack-Hartmann sensor by using astigmatic microlenses," *Optical Engineering, vol.39, no.8,* Aug. 2000, pp.2220-5. SPIE, USA.

4. N. Lindlein, J. Pfund, J. Schwider, "Algorithm for expanding the dynamic range of a Shack-Hartmann sensor by using a spatial light modulator array," *Optical Engineering, vol.40, no.5,* May 2001, pp.837-40. SPIE, USA

5. H. Choo and R. S. Muller, "Optical properties of microlenses fabricated using hydrophobic effects and polymer-jet-printing technology," *2003 IEEE/LEOS International Conference on Optical MEMS and Their Applications,* August 18-21, 2003, pp.169-170. Waikoloa Beach Marriot, Waikoloa, Hawaii